



Article

Low-Melting Manganese(II)-Based Ionic Liquids: Syntheses, Structures, Properties and Influence of Trace Impurities

Tim Peppel ^{1,*} , Monika Geppert-Rybczyńska ², Christin Neise ^{3,4}, Udo Kragl ^{4,5,6}  and Martin Köckerling ^{3,5,*}

¹ Leibniz-Institut für Katalyse e.V. (LIKAT), Heterogene Photokatalyse, Albert-Einstein-Str. 29a, 18059 Rostock, Germany

² Instytut Chemii, Uniwersytet Śląski w Katowicach, Szkolna 9, 40-006 Katowice, Poland; monika.geppert-rybczynska@us.edu.pl

³ Institut für Chemie, Anorganische Festkörperchemie, Universität Rostock, Albert-Einstein-Str. 3a, 18059 Rostock, Germany; christin.neise@gmx.de

⁴ Institut für Chemie, Technische Chemie, Universität Rostock, Albert-Einstein-Str. 3a, 18059 Rostock, Germany; udo.kragl@uni-rostock.de

⁵ Department Life, Light and Matter, Universität Rostock, 18051 Rostock, Germany

⁶ Leibniz-Institut für Katalyse e.V. (LIKAT), Polymerchemie und Katalyse, Albert-Einstein-Str. 29a, 18059 Rostock, Germany

* Correspondence: tim.peppel@catalysis.de (T.P.); martin.koeckerling@uni-rostock.de (M.K.); Tel.: +49-381-1281-126 (T.P.); +49-381-498-6390 (M.K.)

Received: 24 October 2019; Accepted: 13 November 2019; Published: 15 November 2019



Abstract: The synthesis of more than 10 new magnetic ionic liquids with $[\text{MnX}_4]^{2-}$ anions, $\text{X} = \text{Cl}$, NCS , NCO , is presented. Detailed structural information through single-crystal X-ray diffraction is given for $(\text{DMDIm})[\text{Mn}(\text{NCS})_4]$, $(\text{BnEt}_3\text{N})_2[\text{Mn}(\text{NCS})_4]$, and $\{(\text{Ph}_3\text{P})_2\text{N}\}_2[\text{Mn}(\text{NCO}_4)] \cdot 0.6\text{H}_2\text{O}$, respectively. All compounds consist of discrete anions and cations with tetrahedrally coordinated $\text{Mn}(\text{II})$ atoms. They show paramagnetic behavior as expected for spin-only systems. Melting points are found for several systems below 100°C classifying them as ionic liquids. Thermal properties are investigated using differential scanning calorimetry (DSC) measurements. The physicochemical properties of density, dynamic viscosity, electrolytic conductivity, and surface tension were measured temperature-dependent of selected samples. These properties are discussed in comparison to similar Co containing systems. An increasing amount of bromide impurity is found to affect the surface tension only up to 3.3%.

Keywords: manganese; ionic liquid; crystal structure; physical properties; trace impurities

1. Introduction

For the last 20 years, the ongoing tremendous interest in ionic liquids (ILs) as salts with low melting points is based on their partly unique properties which lead to a variety of possible applications. Therefore, ILs have been thoroughly investigated as systems with large electrochemical windows and liquid ranges, hardly measurable vapor pressures, unusual solubility characteristics, and applications in catalysis [1–15]. ILs containing metal-based complex ions, so-called magnetic ionic liquids (MILs), are a highly investigated subclass of ILs, because they show magnetic response in addition to the characteristics mentioned above [16–20]. Such ILs with paramagnetic transition-metal complex anions have also been assumed to be magnetic and magnetorheological fluids [21–23].

In the last 10 years, we have reported on different classes of transition metal-containing low-melting ILs with complex anions of the 3d metals Cr, Co, and Ni, respectively, of which a series of physicochemical data is available [24–34]. The astonishing results from imidazolium-based ILs containing the $[\text{Co}(\text{NCS})_4]^{2-}$ anion [25] led us to extending our research for new low-melting, transparent ILs which contain tetrahedrally coordinated manganese(II) complex anions which could also be suitable as catalysts in chemical reactions. Since the structural motifs especially for manganese complexes is inexhaustible due to the wide range of possible oxidation states (+I to +VII), our research has been focused on homoleptic Mn(II) complex anions only for better comparison with already known MIL subclasses.

The subclass of compounds with (pseudo)tetrahedrally coordinated $[\text{Mn}^{\text{II}}\text{X}_4]^{2-}$ (X = halide, SCN, OCN) complex anions has been known for more than 100 years [35–43], but crystal and molecular structure investigations are still scarce. In order to get a better understanding of solid-state properties of these salts, it is necessary to investigate their crystal and molecular structures. There has been a study on manganate(II)-based ionic liquids with main focus on physico-optical properties of $[\text{Mn}^{\text{II}}\text{X}_4]^{2-}$ -based systems (X = Cl, Br, NTf_2 [NTf_2 : bis (trifluoromethanesulfonyl) amido]) which are solids at room temperature and no single crystal data has been presented [44].

To the best of our knowledge, crystallographic investigations of imidazolium-based salts containing the $[\text{Mn}^{\text{II}}\text{X}_4]^{2-}$ (X = halide) anions are only known for $(\text{ImH})_2[\text{MnCl}_4] \cdot (\text{ImH})_4[\text{MnCl}_6]$ (ImH = 1 H-imidazolium) [45], $(\text{MImPPy})[\text{MnCl}_4]$ (MImPPy = 1-(3-(1-Methylimidazolium-3-yl) propyl) pyridinium) and $(\text{DMBIm})[\text{MnCl}_4]$ (DMBIm = 1,1'-Butane-1, 4-diylbis (3-methylimidazolium) [46], $(\text{BIm})_2[\text{MnCl}_4]$ (BIm = 1-Butyl-3-methylimidazolium) [47,48] and $(\text{BIm})_2[\text{MnBr}_4]$ [49], respectively. It is obvious that, until now, there has been no single crystal data available for imidazolium-based systems, which contain pseudohalides as ligands in the complex anion $[\text{Mn}^{\text{II}}(\text{NCX})_4]^{2-}$ (X = O, S). There are only few reports on crystal structures of $[\text{Mn}^{\text{II}}(\text{NCS})_4]^{2-}$ containing systems [50–53], and only one single report on the crystal structure of a $[\text{Mn}^{\text{II}}(\text{NCO})_4]^{2-}$ containing system, $[\text{Ni}(\text{bpy})_3][\text{Mn}(\text{NCO})_4] \cdot \text{H}_2\text{O}$ (bpy = 2,2'-bipyridine) [54], respectively.

In this contribution, we report on the synthesis, properties and physicochemical investigation of a series of $\text{A}_x[\text{MnX}_4]$ (A = ammonium-, iminium- and imidazolium-based cation; X = Cl, NCS, NCO) complexes with comparably low melting points. The series was divided into two subclasses: a) non-hygroscopic $\text{A}_x[\text{Mn}(\text{NCS})_4]$ compounds, and b) slightly hygroscopic $\text{A}_x[\text{MnX}_4]$ (X = Cl, NCO) compounds, respectively. All compounds were investigated by means of elemental analysis and mid-infrared (MIR) spectroscopy. The first subclass was further investigated by nuclear magnetic resonance (NMR) spectroscopy to obtain magnetic data. Additional measurements of density, dynamic viscosity, conductivity, and surface tension were done exemplarily for the low-melting non-hygroscopic substance $(\text{EMIm})_2[\text{Mn}(\text{NCS})_4]$ (EMIm = 1-ethyl-3-methylimidazolium). The influence of trace impurities (residual bromide) is also discussed on the basis of the physicochemical properties. Electronic spectra are not presented in detail due to the already existing large amount of such data [33,34,36,55]. The crystal and molecular structures of three compounds, $(\text{DMDIm})[\text{Mn}(\text{NCS})_4]$, $(\text{BnEt}_3\text{N})_2[\text{Mn}(\text{NCS})_4]$, and $\{(\text{Ph}_3\text{P})_2\text{N}\}_2[\text{Mn}(\text{NCO})_4] \cdot 0.6\text{H}_2\text{O}$, respectively, are also presented and discussed.

2. Experimental

2.1. Instrumentation

NMR spectra were recorded on a Avance 250 or Avance 300 spectrometer (Bruker, Billerica, MA, USA) and chemical shifts of the ^1H , and ^{13}C spectra were reported in parts per million (ppm) using the solvent shifts for ^1H and ^{13}C as internal standard ($[\text{D}_6]\text{DMSO}$: ^1H δ = 2.50 ppm, ^{13}C δ = 39.5 ppm; D_2O : ^1H δ = 4.75 ppm; CDCl_3 : ^1H δ = 7.26, ^{13}C δ = 77.0) [55]. Elemental analysis for C, H, N and S was performed on a FlashEA 1112 device (Thermo Fisher Scientific, Waltham, MA, USA). The MIR spectra were recorded by the attenuated total reflectance (ATR) technique on a Nicolet 380 FT-IR spectrometer (Thermo Fisher Scientific, Waltham, MA, USA). Melting points were

determined by differential scanning calorimetry (DSC) measurements with a DSC823^e instrument (Mettler-Toledo, Columbus, OH, USA) in the range -100 to 200 °C at a heating rate of 10 K min⁻¹ (Ar atmosphere, Al crucible) or with a STA 449 F3 Jupiter device (Netzsch, Selb, Germany) in the temperature range 25 to 600 °C at a heating rate of 10 K min⁻¹ (N₂ atmosphere, Al crucible), respectively. Single-crystal X-ray diffraction measurements were made with a Apex X8 diffractometer (Bruker-Nonius, Billerica, MA, USA) equipped with a CCD detector. The measurements were performed with monochromatic Mo-K α radiation ($\lambda = 0.71073$ Å). The preliminary unit-cell data were obtained from the reflection positions of 36 frames, measured in different directions of reciprocal space. After the completion of the data measurements, the intensities were corrected for Lorentz, polarization, and absorption effects with the Bruker-Nonius software [56]. The structure solutions and refinements were performed with the SHELX-97 program package [57]. All of the non-hydrogen atoms were refined anisotropically. The hydrogen atoms were added at idealized positions and refined in riding models. These data can be obtained free of charge from the Cambridge Crystallographic Data Centre: CCDC 834685 for (DMDIm)[Mn(NCS)₄], CCDC 834684 for (BnEt₃N)₂[Mn(NCS)₄], and CCDC 1934913 for {(Ph₃P)₂N}₂[Mn(NCO₄)]·0.6H₂O. Magnetic data were determined by ¹H NMR spectroscopy techniques [58,59]. Molar susceptibilities were corrected by applying Pascal constants [60]. Effective magnetic moments μ_{eff}/μ_B were determined by applying the Langevin equation [61]. Trace impurities ([pseudo]-halides, sulphate) were determined by an ionic chromatography (IC) system equipped with a Alltech 550 model conductivity detector. A Metrosep Anion Dual 2 75/4.6 mm column was employed and the mobile phase consisted of a mixture of 1.3 mmol/L NaHCO₃ and 2.0 mmol/L Na₂CO₃ in pure water with a flow rate of 0.8 mL/min. The column temperature was 25 °C. For sample preparation approximately 100 mg of ionic liquid was weighed into a 100 mL volumetric flask and dissolved in pure water (1:1000). The solution was transferred to a sample vial, manually injected and analysed with the IC system. Water contents were determined by Karl Fischer titration on a TitroLine KF Trace device (SI Analytics, Weilheim, Germany). Densities (ρ) and dynamic viscosities (η) were measured with an Stabinger viscometer SVM 3000 (Anton Paar, Graz, Austria). The specification provided by the manufacturer estimates the reproducibility as 0.35% for viscosities and 5×10^{-4} g·cm⁻³ for densities with repeatability on the level 0.1% and 2×10^{-4} g·cm⁻³ for viscosity and density, respectively. Surface tensions (γ) were measured using the pendant drop method with the DSA 10 Tensiometer with Drop Shape Analysis software (Krüss GmbH, Hamburg, Germany). The instrumental procedures and the experimental details have been published previously [34,62]. The general uncertainty of the method given by the manufacturer is 0.1 mN·m⁻¹. Conductivities (κ) were measured with a Microprocessor Conductivity Meter LF 537 with a Tetracon 96 electrode with the general uncertainty 0.5% (WTW, Weilheim, Germany).

2.2. Materials

All commercially available chemicals were used as received (Sigma-Aldrich, St. Louis, MO, USA, purities >99%). *N*-methylimidazole was freshly distilled from KOH in vacuo before use. Monocationic ionic liquid precursors were prepared by literature procedures [63,64].

K₂[Mn(NCS)₄] was synthesized on a multi-gram level: Manganese(II) chloride (MnCl₂, 10.0 g, 79.5 mmol), potassium thiocyanate (KSCN, 31.7 g, 325.8 mmol) were placed in a round-bottom flask and heated under reflux overnight in 250 mL acetone. The precipitate (KCl) was filtered off and the solvent of the light green filtrate was completely removed in vacuo. The residue was extracted with 100 mL dichloromethane, filtered and the solvent was removed again in vacuo. The purified solid was dried overnight at 120 °C, yielding an almost white hygroscopic powder in high yield (26.5 g, 72.5 mmol, 91%). M.p. 169 °C; elemental analysis for C₄K₂MnN₄S₄: calcd. C 13.2 , N 15.3 , S 35.1 ; found C 15.2 , H 0.5 , N 14.4 , S 36.7 .

AgOCN was freshly precipitated each time prior to use by direct salt metathesis of KOCN with excess AgNO₃ in aqueous solution at room temperature in quantitative yield. The resulting colorless

precipitate was filtered off, thoroughly washed with water, ethanol, diethyl ether and finally dried at 60 °C. Elemental analysis for CAgNO: calcd. C 8.0, N 9.4; found C 7.7, H 0.1, N 9.6.

2.3. Synthesis of $A_n^{x+}[Mn(NCS)_4]^{2-}$

Samples of the general formula $A_n^{x+}[Mn(NCS)_4]^{2-}$ ($n = 2, x = 1$: $A = (BnEt_3N)^+, \{(Ph_3P)_2N\}^+, (EMIm)^+, (BMIm)^+$; $n = 1, x = 2$: $A = (DMDIm)^{2+}$) were prepared by adaptation of a known literature procedure [65] via salt metathesis reaction of 2.05 eq. A^+X^- (2.05 mmol) ($A^+X^- = (BnEt_3N)Cl, \{(Ph_3P)_2N\}Cl, (EMIm)Br, (BMIm)Br$) or 1.05 eq. $A^{2+}X_2^-$ (1.05 mmol) ($A^{2+}X_2^- = (DMDIm)Cl_2$) and 1.00 eq. $K_2[Mn(NCS)_4]$ (1.00 mmol) in 50 mL boiling acetone. The resulting suspensions were refluxed overnight, filtered, afterwards the solvent was removed in vacuo and the residue was washed with portions of dichloromethane. The solvent of the combined filtrates was removed in vacuo yielding light greenish compounds in good yields (>75%).

$(BnEt_3N)_2[Mn(NCS)_4]$, bis (benzyl-triethylammonium) tetrakisothiocyanatomanganate(II): Prepared from commercial $(BnEt_3N)Cl$. Light green solid, yield 90%. M.p. (exp.) 101 °C, glass transition (exp.) −13 °C, $T_g/T_m = 0.70$; elemental analysis for $C_{30}H_{44}MnN_6S_4$ (calcd.): C 54.4 (53.6), H 7.1 (6.6), N 12.4 (12.5), S 18.8 (19.0); IR (ATR, 32 scans, 25 °C, cm^{-1}): 3032, 3005, 2985, 2945, 2873, 2069 (CN str. [65]), 2030, 1495, 1477, 1454, 1392, 1365, 1328, 1211, 1152, 1082, 1007, 966, 941, 902, 829 (CS str. [65]), 811, 793, 776, 751, 703, 604, 536.

$\{(Ph_3P)_2N\}_2[Mn(NCS)_4]$, bis-(bis (triphenylphosphine) iminium) tetrakisothiocyanatomanganate(II): Prepared from commercial $\{(Ph_3P)_2N\}Cl$. Greenish solid, yield 94%. M.p. (exp.) 144 °C, glass transition (exp.) 55 °C, $T_g/T_m = 0.79$; elemental analysis for $C_{76}H_{60}MnN_6P_4S_4$ (calcd.): C 66.7 (66.9), H 4.4 (4.4), N 6.2 (6.2), S 9.5 (9.4); IR (ATR, 32 scans, 25 °C, cm^{-1}): 3144, 2983, 2955, 2872, 2037 (CN str. [65]), 1567, 1444, 1430, 1330, 1290, 1261, 1163, 1100, 1090, 960, 825 (CS str. [65]), 739, 700, 643, 620, 598.

$(EMIm)_2[Mn(NCS)_4]$, bis (1-ethyl-3-methylimidazolium) tetrakisothiocyanatomanganate(II): Prepared from $(EMIm)Br$ [66]. Green liquid, yield 76%. glass transition (exp.) −57 °C, M.p. (calcd.) 51 °C; elemental analysis for $C_{16}H_{22}MnN_8S_4$ (calcd.): C 37.5 (37.7), H 4.1 (4.3), N 20.6 (21.9), S 22.3 (25.1); IR (ATR, 32 scans, 25 °C, cm^{-1}): 3145, 3103, 2982, 2953, 2874, 2036 (CN str. [65]), 1565, 1446, 1425, 1385, 1334, 1291, 1261, 1163, 1105, 1086, 1029, 958, 827 (CS str. [65]), 740, 700, 644, 618, 596; $\mu_{eff} = 5.9 \mu_B$ ($T = 25$ °C, $c = 49.0$ mmol/L, $\nu_0 = 300$ MHz, $\chi_{mol} = 14.6 \times 10^{-3}$).

$(BMIm)_2[Mn(NCS)_4]$, bis (1-butyl-3-methylimidazolium) tetrakisothiocyanatomanganate(II): Prepared from $(BMIm)Br$ [67]. Green liquid, yield 77%. glass transition (exp.) −58 °C, M.p. (calcd.) 50 °C; elemental analysis for $C_{24}H_{30}MnN_8S_4$ (calcd.): C 43.6 (42.5), H 5.6 (5.4), N 19.7 (19.8), S 22.9 (22.7); IR (ATR, 32 scans, 25 °C, cm^{-1}): 3143, 3104, 2958, 2932, 2872, 2040 (CN str. [65]), 1563, 1461, 1425, 1380, 1336, 1278, 1207, 1162, 1105, 1087, 1022, 963, 824 (CS str. [65]), 740, 696, 647, 618; $\mu_{eff} = 6.0 \mu_B$ ($T = 25$ °C, $c = 42.4$ mmol/L, $\nu_0 = 300$ MHz, $\chi_{mol} = 15.1 \times 10^{-3}$).

$(DMDIm)[Mn(NCS)_4]$, 3,3'-methylenbis (1-methyl-imidazolium) tetrakisothiocyanatomanganate(II): Prepared from $(DMDIm)Cl_2$ [34]. Light green solid, yield 86%. M.p. (exp.) 179 °C, glass transition (exp.) 26 °C, $T_g/T_m = 0.66$; elemental analysis for $C_{13}H_{14}MnN_8S_4$ (calcd.): C 30.7 (33.5), H 2.5 (3.0), N 22.0 (24.0), S 27.5 (27.6); IR (ATR, 32 scans, 25 °C, cm^{-1}): 3150, 3130, 3098, 3070, 2092, 2054 (CN str. [65]), 1699, 1599, 1558, 1546, 1427, 1367, 1321, 1234, 1160, 1081, 958, 838, 827 (CS str. [65]), 765, 749, 732, 673, 620, 602, 536.

2.4. Synthesis of $A_n^{x+}[MnCl_4]^{2-}$

Samples of the general formula $A_2^{+}[MnCl_4]^{2-}$ ($A = (BnEt_3N)^+, \{(Ph_3P)_2N\}^+, (EMIm)^+, (BMIm)^+$) were prepared by adaptation of a known literature procedures [37,41] via direct reaction of 2.05 eq. A^+X^- (2.05 mmol) ($A^+X^- = (BnEt_3N)Cl, \{(Ph_3P)_2N\}Cl, (EMIm)Cl, (BMIm)Cl$) or 1.05 eq. $A^{2+}X_2^-$ (1.05 mmol) ($A^{2+}X_2^- = (DMDIm)Cl_2$) and 1.00 eq. anhydrous $MnCl_2$ (1.00 mmol) in 50 mL boiling ethanol. The resulting suspensions were refluxed for 30 min, cooled down to room temperature

and the solvent was removed in vacuo. The residue was washed thoroughly with portions of ethyl acetate/ethanol (1:1) and diethyl ether and dried in vacuo yielding light greenish to yellow slightly hygroscopic substances in good to excellent yields (>80%).

(BnEt₃N)₂[MnCl₄], bis (benzyl-triethylammonium) tetrachloridomanganate(II): Prepared from commercial (BnEt₃N)Cl. White hygroscopic solid, yield 84%. M.p. (exp.) 106 °C, glass transition (exp.) 13 °C, $T_g/T_m = 0.75$; elemental analysis for C₂₆H₄₄MnN₂Cl₄ (calcd.): C 54.0 (53.7), H 7.6 (7.6), N 4.9 (4.8); IR (ATR, 32 scans, 25 °C, cm⁻¹): 3500, 3444, 3191, 2987, 2944, 1604, 1498, 1480, 1456, 1448, 1480, 1406, 1394, 1371, 1332, 1297, 1210, 1196, 1184, 1155, 1077, 1030, 1009, 941, 903, 808, 777, 752, 708, 699, 613, 604, 547, 537.

{(Ph₃P)₂N}₂[MnCl₄], bis-(bis (triphenylphosphine) iminium) tetrachloridomanganate(II): Prepared from commercial {(Ph₃P)₂N}Cl. White hygroscopic solid, yield 93%. M.p. (exp.) 240 °C, glass transition (exp.) 75 °C, $T_g/T_m = 0.68$; elemental analysis for C₇₂H₆₀MnN₂P₄Cl₄ (calcd.): C 66.6 (67.9), H 4.8 (4.8), N 2.3 (2.2); IR (ATR, 32 scans, 25 °C, cm⁻¹): 3261, 3054, 2414, 2351, 2141, 1949, 1587, 1435, 1223, 1112, 1104, 1026, 997, 933, 877, 848, 800, 746, 721, 689, 550, 528.

(EMIm)₂[MnCl₄], bis (1-methyl-3-methylimidazolium) tetrachloridomanganate(II): Prepared from commercial (EMIm)Cl. Greenish hygroscopic solid, yield 94%. M.p. (exp.) 133 °C (lit. 130 °C [68]), elemental analysis for C₁₂H₂₂MnN₄Cl₄ (calcd.): C 34.6 (34.4), H 5.5 (5.3), N 13.3 (13.4); IR (ATR, 32 scans, 25 °C, cm⁻¹): 3140, 3097, 3060, 2960, 2934, 2875, 1738, 1731, 1715, 1651, 1644, 1633, 1614, 1565, 1463, 1446, 1432, 1380, 1338, 1322, 1305, 1280, 1261, 1202, 1164, 1114, 1088, 1067, 1048, 1028, 976, 950, 862, 846, 800, 765, 728, 661, 655, 621.

(BMIm)₂[MnCl₄], bis (1-butyl-3-methylimidazolium) tetrachloridomanganate(II): Prepared from (BMIm)Cl [63]. Greenish hygroscopic solid, yield 92%. M.p. (exp.) 67 °C (lit. 62–63 °C [44,47]), elemental analysis for C₁₆H₃₀MnN₄Cl₄ (calcd.): C 40.3 (40.4), H 6.3 (6.4), N 11.6 (11.8); IR (ATR, 32 scans, 25 °C, cm⁻¹): 3140, 3097, 3060, 2960, 2934, 2875, 1738, 1731, 1715, 1651, 1644, 1633, 1614, 1565, 1463, 1446, 1432, 1380, 1338, 1322, 1305, 1280, 1261, 1202, 1164, 1114, 1088, 1067, 1048, 1028, 976, 950, 862, 846, 800, 765, 728, 661, 655, 621.

(DMDIm)[MnCl₄], 3,3'-methylenbis (1-methyl-imidazolium) tetrachloridomanganate(II): Prepared from (DMDIm)Cl₂ [34]. Greenish hygroscopic solid, yield 80%. M.p. (exp.) 315 °C, elemental analysis for C₉H₁₄MnN₄Cl₄ (calcd.): C 28.9 (28.8), H 3.7 (3.8), N 14.8 (14.9); IR (ATR, 32 scans, 25 °C, cm⁻¹): 3140, 3097, 3060, 2960, 2934, 2875, 1738, 1731, 1715, 1651, 1644, 1633, 1614, 1565, 1463, 1446, 1432, 1380, 1338, 1322, 1305, 1280, 1261, 1202, 1164, 1114, 1088, 1067, 1048, 1028, 976, 950, 862, 846, 800, 765, 728, 661, 655, 621.

2.5. Synthesis of A₂⁺[Mn(NCO)₄]²⁻

Samples of the general formula A₂⁺[Mn(NCO)₄]²⁻ (A = (BnEt₃N)⁺, {(Ph₃P)₂N}⁺, (BMIm)⁺) were prepared by adaptation of a known literature procedure [42] via salt metathesis reaction of 4.05 eq. freshly precipitated AgOCN (4.05 mmol) and 1.00 eq. A₂⁺[MnCl₄]²⁻ (1.00 mmol) in 50 mL boiling nitromethane. The resulting suspensions were refluxed overnight, filtered, afterwards the solvent was removed in vacuo and the residue was washed with portions of dichloromethane. The solvent of the combined filtrates was removed in vacuo yielding light greenish powders or solids in moderate to excellent yields (70–95%).

(BnEt₃N)₂[Mn(NCO)₄], bis (benzyl-triethylammonium) tetrakisocyanatomanganate(II): Prepared from (BnEt₃N)₂[MnCl₄] (see above). Light green slightly hygroscopic liquid, yield 73%; elemental analysis for C₃₀H₄₄MnN₆O₄: C 56.6 (58.4), H 7.1 (7.4); N 13.3 (13.6); IR (ATR, 32 scans, 25 °C, cm⁻¹): 3503, 2989, 2218, 2172 (CN str. [[69]]), 1712, 1584, 1556, 1498, 1479, 1455, 1395, 1366, 1328 (CO str. [69]), 1300, 1258, 1213, 1184, 1173, 1154, 1100, 1081, 1029, 1006, 942, 902, 857, 830, 791, 753, 704, 656, 622 (NCO bend. [69]), 605, 537.

{(Ph₃P)₂N}₂[Mn(NCO)₄], bis (bis (triphenylphosphine) iminium) tetrakisocyanatomanganate(II): Prepared from {(Ph₃P)₂N}₂[MnCl₄] (see above). orange solid, yield 95%. M.p. (exp.) 200 °C; elemental analysis for C₆₈H₆₀MnN₆O₄P₄: C 67.2 (67.8), H 4.7 (5.0), N 7.0 (7.0); IR (ATR, 32 scans, 25 °C, cm⁻¹): 3507, 3059, 2219, 2187 (CN str. [69]), 2139, 2046, 1973, 1588, 1563, 1557, 1483, 1437, 1402, 1332 (CO str. [69]), 1297, 1279, 1242, 1177, 1164, 1109, 1074, 1028, 997, 935, 847, 803, 760, 746, 721, 688, 621 (NCO bend. [69]), 552, 528.

(EMIm)₂[Mn(NCO)₄], bis (1-methyl-3-methylimidazolium) tetrakisocyanatomanganate(II): Prepared from (EMIm)₂[MnCl₄] (see above). Light yellow-green liquid, yield 80%. glass transition (exp.) −82 °C, M.p. (calcd.) 13 °C; elemental analysis for C₁₆H₂₂MnN₈O₄ (calcd.): C 43.1 (43.1), H 4.4 (5.0), N 23.9 (25.2); IR (ATR, 32 scans, 25 °C, cm⁻¹): 3506, 3148, 3109, 2961, 2935, 2874, 2175 (CN str. [69]), 1713, 1565, 1463, 1427, 1330 (CO str. [69]), 1227, 1164, 1109, 1090, 1023, 948, 842, 751, 698, 651, 619 (NCO bend. [69]).

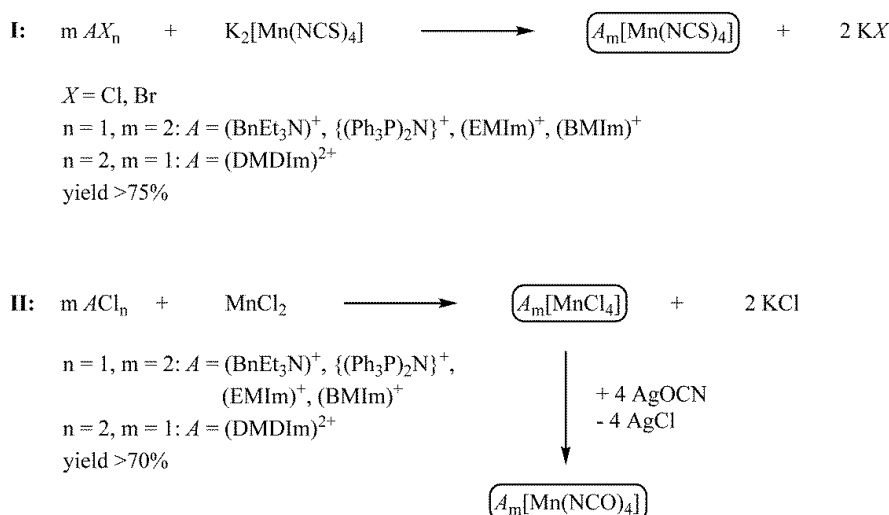
(BMIm)₂[Mn(NCO)₄], bis (1-butyl-3-methylimidazolium) tetrakisocyanatomanganate(II): Prepared from (BMIm)₂[MnCl₄] (see above). Light green slightly hygroscopic liquid, yield 71%. glass transition (exp.) −80 °C, M.p.(calcd.) 16 °C; elemental analysis for C₂₀H₃₀MnN₈O₄ (calcd.): C 47.4 (47.9), H 5.5 (6.0), N 20.8 (22.3); IR (ATR, 32 scans, 25 °C, cm⁻¹): 3506, 3148, 3109, 2961, 2935, 2874, 2175 (CN str. [69]), 1713, 1565, 1463, 1427, 1330 (CO str. [69]), 1227, 1164, 1109, 1090, 1023, 948, 842, 751, 698, 651, 619 (NCO bend. [69]).

(DMDIm)[Mn(NCO)₄], 3,3'-methylenebis (1-methyl-imidazolium) tetrakisocyanatomanganate(II): Prepared from (DMDIm)[MnCl₄] (see above). Greenish hygroscopic solid, yield 82%. M.p.(exp.) 132 °C, elemental analysis for C₁₃H₁₄MnN₄O₄ (calcd.): C 38.1 (38.9), H 3.5 (3.5), N 27.4 (27.9); IR (ATR, 32 scans, 25 °C, cm⁻¹): 3506, 3148, 3109, 2961, 2935, 2874, 2175 (CN str. [69]), 1713, 1565, 1463, 1427, 1330 (CO str. [69]), 1227, 1164, 1109, 1090, 1023, 948, 842, 751, 698, 651, 619 (NCO bend. [69]).

3. Results and Discussion

3.1. Syntheses

The schematic synthetic approach to obtain low-melting salts consisting of [MnX₄]²⁻ complex anions (X = Cl, NCS, NCO) is depicted in Scheme 1.



Scheme 1. General synthetic approach for the synthesis of [Mn(NCS)₄]²⁻-based (I) and [MnX₄]²⁻-based salts (X = Cl, NCO; II).

[Mn(NCS)₄]²⁻-based compounds were synthesized by well-established salt metathesis reactions of ammonium-, iminium- or imidazolium-based halide salts with K₂[Mn(NCS)₄] (generated from the

reaction of KSCN and MnCl_2 to generate compounds of the composition $\text{A}_n^{x+}[\text{Mn}(\text{NCS})_4]^{2-}$ ($n = 2$: $\text{A} = (\text{BnEt}_3\text{N})^+$, $\{(\text{Ph}_3\text{P})_2\text{N}\}^+$, $(\text{EMIm})^+$, $(\text{BMIm})^+$; $n = 1$: $\text{A} = (\text{DMDIm})^{2+}$) in moderate to high yields (see Scheme 1I). The compound with one of the lowest glass transition points, $(\text{EMIm})_2[\text{Mn}(\text{NCS})_4]$ ($T_g = -57\text{ }^\circ\text{C}$) was chosen exemplarily for further physicochemical investigations on corresponding densities (ρ), dynamic viscosities (η), surface tensions (γ) and conductivities (κ), respectively, and it was synthesized for this purpose at the multi-gram scale ($\sim 100\text{--}250\text{ mL IL}$). The reactions were performed in acetonic solutions to ensure complete precipitation of the side product KX ($\text{X} = \text{Cl}, \text{Br}$).

$[\text{MnX}_4]^{2-}$ -based compounds ($\text{X} = \text{Cl}, \text{NCO}$) were synthesized in a two-step reaction pathway by direct reaction of ammonium-, iminium- or imidazolium-based chloride salts with MnCl_2 in ethanol solution and further ligand exchange reaction with freshly prepared AgOCN in nitromethane to generate $[\text{Mn}(\text{NCO})_4]^{2-}$ -based complexes (see Scheme 1II). The respective chlorido- as well as isocyanato complexes show significant tendencies to deliquesce.

3.2. Crystal Structures

Single crystals suitable for X-ray structure determinations of $(\text{DMDIm})[\text{Mn}(\text{NCS})_4]$, $(\text{BnEt}_3\text{N})_2[\text{Mn}(\text{NCS})_4]$, and $\{(\text{Ph}_3\text{P})_2\text{N}\}_2[\text{Mn}(\text{NCO})_4] \cdot 0.6\text{H}_2\text{O}$ were obtained by slow evaporation of the solvents, for example acetonitrile, of solutions of the three compounds at ambient pressure and temperatures of $25\text{ }^\circ\text{C}$. All consist of discrete $[\text{Mn}(\text{NCX})_4]^{2-}$ anions ($\text{X} = \text{S}$ or O) and the organic N-based cation. Figures 1–3 show the molecular structures of the 3 compounds.

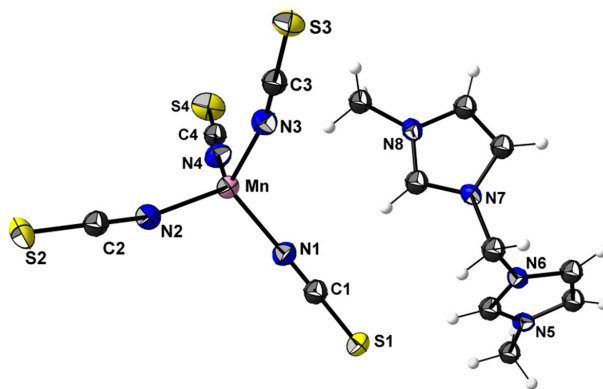


Figure 1. Molecular structure of $(\text{DMDIm})[\text{Mn}(\text{NCS})_4]$ with labeling of selected atoms. Thermal displacement ellipsoids are drawn at the 50% probability level.

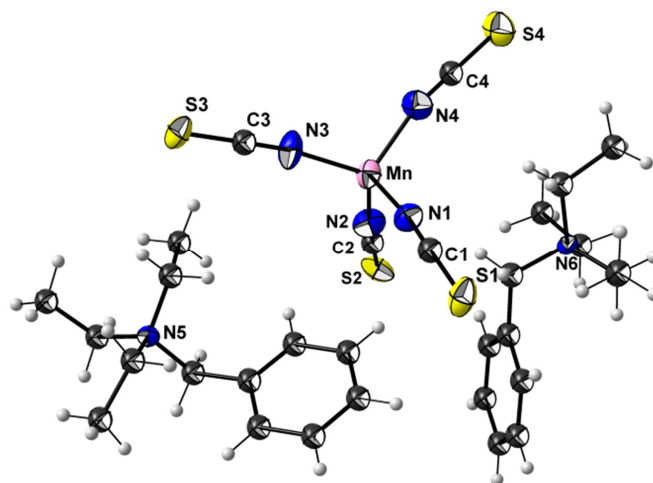


Figure 2. Molecular structure of $(\text{BnEt}_3\text{N})_2[\text{Mn}(\text{NCS})_4]$ with labeling of selected atoms. Thermal displacement ellipsoids are drawn at the 50% probability level.

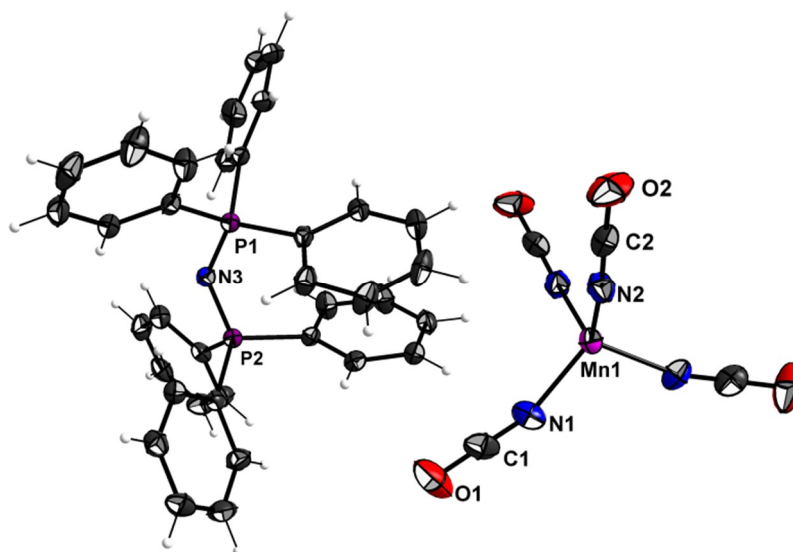


Figure 3. Molecular structure of $((\text{Ph}_3\text{P})_2\text{N})_2[\text{Mn}(\text{NCO})_4]$ with labeling of selected atoms. Thermal displacement ellipsoids are drawn at the 50% probability level.

All atom distances and angles as well as all the other crystallographic and structure determination parameters are deposited with the CCDC (see Experimental Section). The bond distances and angles are found within the expected ranges. The cations and anions are located on general positions with the exception of the anion in $\{(\text{Ph}_3\text{P})_2\text{N}\}_2[\text{Mn}(\text{NCO})_4]$, which is located on the Wyckoff site 2a with twofold rotational symmetry. In all cases the Mn atoms have a tetrahedral MnN_4 coordination environment with some deviations of the N-Mn-N angle from the ideal tetrahedral value. The ranges are $100.82(7)^\circ$ – $112.60(7)^\circ$ in $(\text{DMDIm})[\text{Mn}(\text{NCS})_4]$, $104.24(8)^\circ$ – $116.83(9)^\circ$ in $(\text{BnEt}_3\text{N})_2[\text{Mn}(\text{NCS})_4]$, and $104.2(1)^\circ$ – $113.9(1)^\circ$ in $\{(\text{Ph}_3\text{P})_2\text{N}\}_2[\text{Mn}(\text{NCO})_4]$. These values average at the ideal tetrahedral angle.

3.3. Thermal and Magnetic Properties

Thermal properties of all compounds were measured by using DSC techniques in the temperature range -100 to 600°C in order to investigate melting points as well as glass transitions. DSC measurements were performed in a three cycle repetition mode. All solid materials were heated above their melting points, then cooled down to -100°C and again heated up showing in some cases additional glass transitions prior re-crystallization and melting behavior.

The ratio of melting point (T_m) and glass transition temperature (T_g) was calculated for those compounds which showed melting and glass transitions in the DSC experiments, for example $(\text{DMDIm})[\text{Mn}(\text{NCS})_4]$: $T_m = 179^\circ\text{C}$ (452.15 K), $T_g = 26^\circ\text{C}$ (299.15 K); $T_g/T_m = 0.66$. These values resemble closely the empirical relationship ($T_g/T_m = 2/3 \approx 0.67$ [70,71]) which can be found for a variety of glassy and supercooled systems. The corresponding melting points were calculated on this assumption for all other compounds which showed glass transition behavior only. All observed transitions (melting points and glass transitions) as well as calculated values are listed in detail in the Experimental Section for each compound.

In general, the melting point of candidates from all three subclasses of $[\text{MnX}_4]^{2-}$ -based compounds ($X = \text{Cl}, \text{NCS}, \text{NCO}$) can be found below or near the arbitrarily chosen limit for room-temperature ionic liquids (RTILs) of 100°C , for example $(\text{BnEt}_3\text{N})_2[\text{MnCl}_4]$: 106°C ; $(\text{BnEt}_3\text{N})_2[\text{Mn}(\text{NCS})_4]$: 101°C ; $(\text{BIm})_2[\text{Mn}(\text{NCO})_4]$: $\sim 16^\circ\text{C}$ (calcd.). Interestingly, the already relatively low melting point of $(\text{BIm})_2[\text{MnCl}_4]$ (67°C) is even higher by $\sim 17\text{ K}$ than that of $(\text{BIm})_2[\text{Mn}(\text{NCS})_4]$ with $T_{m,\text{calc.}} \sim 50^\circ\text{C}$ or $\sim 51\text{ K}$ of $(\text{BIm})_2[\text{Mn}(\text{NCO})_4]$ with $T_{m,\text{calc.}} \sim 16^\circ\text{C}$. This lowering of the melting point is achieved by exchange from chlorido- to isothiocyanato-, or isocyanato ligands, respectively. The lowest glass transition temperature was detected for $(\text{EIm})_2[\text{Mn}(\text{NCO})_4]$ with $T_g = -82^\circ\text{C}$. This behavior is in accordance with comparable $[\text{Co}(\text{NCX})_4]^{2-}$ -based systems ($X = \text{S}, \text{O}$) [34].

Magnetic properties at room temperature ($T = 25\text{ }^{\circ}\text{C}$) were measured $(\text{EMIm})_2[\text{Mn}(\text{NCS})_4]$ and $(\text{BMIm})_2[\text{Mn}(\text{NCS})_4]$, respectively, by applying NMR techniques [58,59]. Both complexes show magnetic moments in the range of $\mu_{\text{eff}} = 5.9\text{--}6.0\text{ }\mu_{\text{B}}$ which resembles closely to the spin only value ($\mu_{\text{eff}} = 5.92\text{ }\mu_{\text{B}}$) and experimental data of comparable tetrahedral high-spin Mn^{II} complexes, for example $(^n\text{BuPh}_3\text{P})_2[\text{Mn}(\text{NCS})_4]$ ($\mu_{\text{eff}} = 5.92\text{ }\mu_{\text{B}}$, 296 K [65]), $(\text{Ph}_2\text{MeAs})_2[\text{MnCl}_4]$ ($\mu_{\text{eff}} = 5.88\text{ }\mu_{\text{B}}$, 20 $^{\circ}\text{C}$ [39]), $(\text{Et}_4\text{N})_2[\text{Mn}(\text{NCO})_4]$ ($\mu_{\text{eff}} = 5.98\text{ }\mu_{\text{B}}$, 296 K [42]).

3.4. Physicochemical Properties and Influence of Trace Impurities

The impact of water content on physicochemical properties of ILs is known and has been investigated in detail for a long time [72–74], but the analyses led to in part opposite results. For example, the basic estimations of contents of water and other impurities in ILs have deficiencies in different applied methods and apparatuses with different and relatively large uncertainties ($\sim 10\%$). In general, it is known that the influence of water depends strongly of the nature of the ILs and their structures. The situation for viscosities and conductivities is even more complex, but a general trend is known: The higher the water content in aprotic ILs, the lower the viscosities and higher the conductivities. If the water content is below 0.1% an impact of 5%–15% could be detected [72,73]. More recently, the influence of water was also investigated on the speed of sound and antielectrostatic activity in ILs [75,76]. The findings showed that the water content differed significantly from IL to IL at a really low level. The surface tension and densities were not affected significantly and were in agreement with earlier observations [73]. Further insights for such phenomena with regard of the influence of water on properties of ILs were done by theoretical investigations [77].

The physicochemical properties of three $(\text{EMIm})_2[\text{Mn}(\text{NCS})_4]$ samples (I: 0.006, II: 0.060, III: 0.120 $\text{mol}\cdot\text{dm}^{-3}$) were investigated for their respective densities (ρ), dynamic viscosities (η), electrolytic conductivities (κ) and surface tensions (γ) in the general temperature range (288.15–323.15) K (step: 5 K). Surface tension measurements were limited to 318.15 K and the water content in all samples was below 200 ppm. From obvious reasons, the results for sample I are discussed in details. Results of all measurements are depicted in Figures 4 and 5, respectively.

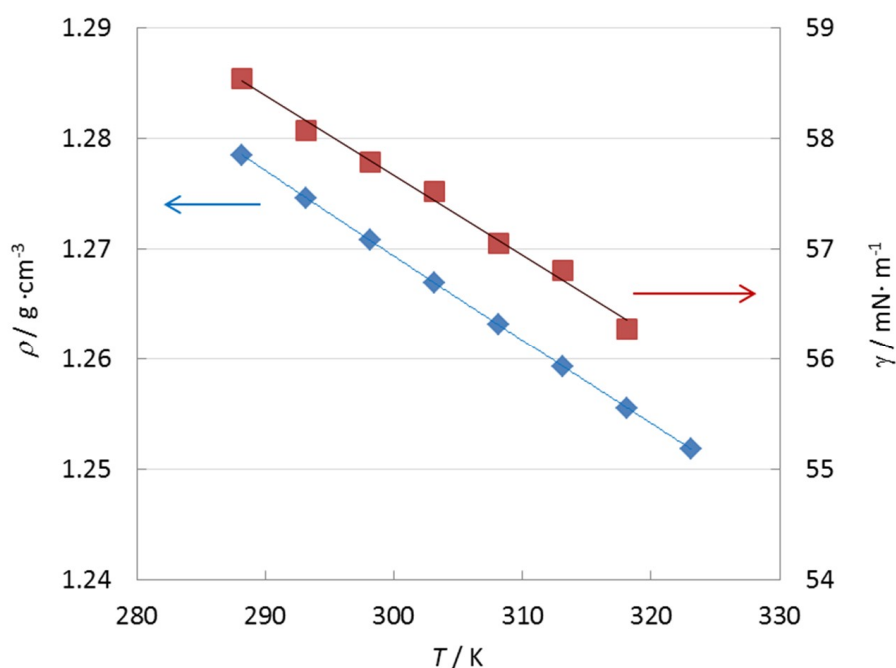


Figure 4. Density (blue squares/line) and surface tension (red squares/line) of $(\text{EMIm})_2[\text{Mn}(\text{NCS})_4]$ (sample I) at different temperatures T .

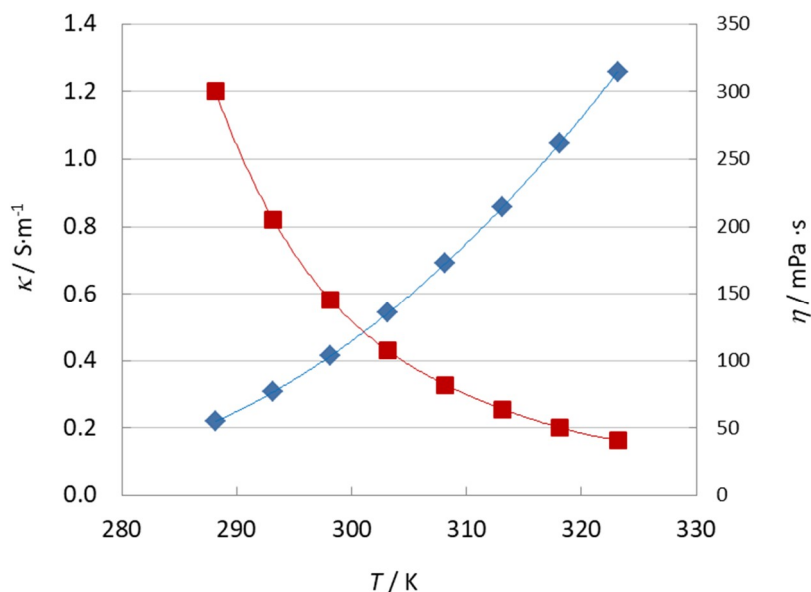


Figure 5. Electrolytic conductivity (blue squares/line) and dynamic viscosity (red squares/line) of (EMIm)₂[Mn(NCS)₄] (sample I) at different temperatures T.

The density of all investigated samples is very similar despite of different bromide content and the maximum relative deviation at 298.15 K between samples I and III is −0.3%. The Mn(II)-based ionic liquids have lower density (for sample I: 1.2707 g·cm^{−3} at 298.15 K) than similar ILs with the same cation (EMIm)⁺ and [Co(NCO)₄]^{2−} or [Co(NCS)₄]^{2−} anions (1.2981 and 1.2839 g·cm^{−3} at 298.15 K, respectively [25,34].

The maximum deviations for surface tension at 298.15 K between samples I and III is 3.3% and the surface tension of sample I of (EMIm)₂[Mn(NCS)₄] (57.8 mN·m^{−1}) is similar to the γ value for (EMIm)₂[Co(NCS)₄] (55.37 mN·m^{−1}) [25].

The agreement between electrolytic conductivity and viscosity for all three investigated samples is very surprising (the maximum deviation is 7.2% and −8.8%, for conductivity and for viscosity, respectively). Furthermore, at 298.15 K the conductivity and dynamic viscosity of (EMIm)₂[Mn(NCS)₄] (0.414 S·m^{−1}; 145.8 mPa·s) is very similar to comparable values of (EMIm)₂[Co(NCS)₄] (0.4 S·m^{−1}; 145.4 mPa·s) [25].

In summary, the variation of bromide content on the level investigated in this work does not affect seriously measured parameters. The most interesting fact is that all investigated properties for (EMIm)₂[Mn(NCS)₄] mirror the proper values found earlier for (EMIm)₂[Co(NCS)₄] [25].

The temperature dependence of the density of the sample I is as follows:

$$\rho / (\text{g} \cdot \text{cm}^{-3}) = 1.4984 - 7.63 \times 10^{-4} \cdot T / \text{K} \quad (s = 0.7 \times 10^{-4} \text{ g} \cdot \text{cm}^{-3})$$

where as the temperature dependence of surface tension is:

$$\sigma / (\text{mN} \cdot \text{m}^{-1}) = 79.3 - 72 \times 10^{-3} \cdot T / \text{K} \quad (s = 0.08 \text{ mN} \cdot \text{m}^{-1}).$$

On the basis of the first dependence the isobaric coefficient of thermal expansion, $\alpha_p = 1/V \cdot (\partial V / \partial T)_p = -1/\rho \cdot (\partial \rho / \partial T)_p$ was calculated and compared with α_p for other (EMIm)⁺ salts with [Co(NCX)₄]^{2−} (X = O, S) complex anions (see Figure 6).

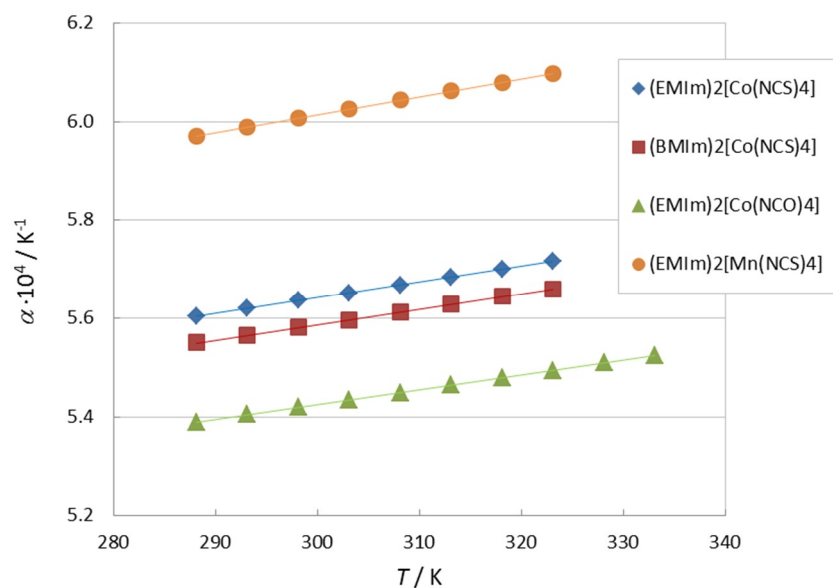


Figure 6. Isobaric coefficient of thermal expansion of (EMIm)₂[Mn(NCS)₄] (sample I, orange dots/line) compared to (EMIm)₂[Co(NCS)₄] [25] (blue squares/line) and (EMIm)₂[Co(NCO)₄] [34] (green triangles/line).

α_p of (EMIm)₂[Mn(NCS)₄] is significantly higher than the other regarded (EMIm)⁺-based ionic liquids.

The temperature dependence of surface tension allowed to obtain the surface entropy $S^a = -(\partial\gamma/\partial T)_p$, which is for (EMIm)₂[Mn(NCS)₄] equal $72 \times 10^{-6} \text{ J}\cdot\text{m}^{-2}\cdot\text{K}^{-1}$. This value is much lower than for other substances taken for comparisons such as (EMIm)₂[Co(NCO)₄] with $S^a = 90.01 \times 10^{-6} \text{ J}\cdot\text{m}^{-2}\cdot\text{K}^{-1}$ [34] and (EMIm)₂[Co(NCS)₄] with $S^a = 99.4 \times 10^{-6} \text{ J}\cdot\text{m}^{-2}\cdot\text{K}^{-1}$ [25] and denotes higher surface order for the investigated (EMIm)₂[Mn(NCS)₄] IL.

The temperature dependence of viscosity and electric conductivity was described using a Vogel–Fulcher–Tamman (VTF) type of equation [78–80]:

$$x = x_0 \cdot \exp(B/(T - T_0))$$

where x is η (mPa·s) or κ (S·m^{−1}); x_0 -pre-exponential factors η_0 and κ_0 (in units as regarded transport quantities); B is a material constant and T_0 is temperature of an ideal glass transition. Fitting parameters x_0 , B and T_0 are collected in Table 1.

Table 1. Fitting parameters of Vogel–Fulcher–Tamman (VTF) equations applied to the viscosity and the electrolytic conductivity of (EMIm)₂[Mn(NCS)₄] (sample I).

$\eta_0/(\text{mPa}\cdot\text{s})$	B/K	T_0/K	r
0.348 ± 0.034	570 ± 20	204 ± 2	0.999996
$\kappa_0/(\text{S}\cdot\text{m}^{-1})$	B/K	T_0/K	r
72.4 ± 4.5	-471 ± 13	206.9 ± 1.4	0.999996

The value of T_0 obtained for (EMIm)₂[Mn(NCS)₄] (sample I) from conductivity (see Table 1) agrees very well with the value from viscosity. Generally, the temperature of an ideal glass transition for all (EMIm)⁺-based ionic liquids calculated based on temperature dependence of conductivity are very close (208(5) K and 206.5(1.4) K for (EMIm)₂[Co(NCS)₄] and (EMIm)₂[Co(NCO)₄], respectively) [25,34]. However, T_0 calculated from viscosity reveals some kind of variation: It is the

lowest for (EMIm)₂[Co(NCS)₄] (172(12) K [25]) and higher for (EMIm)₂[Co(NCO)₄] (190.4(0.2) K [34]). Thus, the highest T_0 from viscosity has (EMIm)₂[Mn(NCS)₄] (sample I) investigated in this work.

Author Contributions: Conceptualization, T.P. and M.K.; methodology, T.P. and M.G.-R.; validation, T.P., M.G.-R. and M.K.; formal analysis, C.N., M.G.-R. and M.K.; investigation, M.G.-R. and C.N.; resources, M.K. and U.K.; Writing—Original draft preparation, T.P., M.G.-R. and M.K.; Writing—Review and editing, T.P. and M.K.; visualization, T.P., M.G.-R. and M.K.; supervision, M.K.

Funding: Support from the Deutsche Forschungsgemeinschaft (Priority Program SPP 1191-Ionic Liquids, KO-1616/4-1 and 1616/4-2, and KR 2491/8-1 and 2491/8-2) is gratefully acknowledged.

Acknowledgments: The authors gratefully acknowledge Jochen K. Lehmann (University of Rostock), Sebastian Przymusiński (University of Rostock) and Thomas Fahrenwaldt (University of Rostock) for their helpful support and discussion. Angela Weihs (University of Rostock) and Alexander Wotzka (LIKAT) and gratefully acknowledged for performing DSC measurements.

Conflicts of Interest: The authors declare no conflict of interest.

References

1. Welton, T. Room-temperature ionic liquids. Solvents for synthesis and catalysis. *Chem. Rev.* **1999**, *99*, 2071–2083. [[CrossRef](#)] [[PubMed](#)]
2. Hallett, J.P.; Welton, T. Room-temperature ionic liquids: Solvents for synthesis and catalysis. 2. *Chem. Rev.* **2011**, *111*, 3508–3576. [[CrossRef](#)] [[PubMed](#)]
3. Wasserscheid, P.; Keim, W. Ionic liquids—New “solutions” for transition metal catalysis. *Angew. Chem. Int. Ed.* **2000**, *39*, 3772–3789. [[CrossRef](#)]
4. Earle, M.J.; Seddon, K.R. Ionic liquids. Green solvents for the future. *Pure Appl. Chem.* **2000**, *72*, 1391–1398. [[CrossRef](#)]
5. Sheldon, R. Catalytic reactions in ionic liquids. *Chem. Commun.* **2001**, 2399–2407. [[CrossRef](#)]
6. Galinski, M.; Lewandowski, A.; Stepniak, I. Ionic liquids as electrolytes. *Electrochim. Acta* **2006**, *51*, 5567–5580. [[CrossRef](#)]
7. Parvulescu, V.I.; Hardacre, C. Catalysis in ionic liquids. *Chem. Rev.* **2007**, *107*, 2615–2665. [[CrossRef](#)]
8. Plechkova, N.V.; Seddon, K.R. Applications of ionic liquids in the chemical industry. *Chem. Soc. Rev.* **2008**, *37*, 123–150. [[CrossRef](#)]
9. MacFarlane, D.R.; Tachikawa, N.; Forsyth, M.; Pringle, J.M.; Howlett, P.C.; Elliott, G.D.; Davis, J.H.; Watanabe, M.; Simon, P.; Angell, C.A. Energy applications of ionic liquids. *Energy Environ. Sci.* **2014**, *7*, 232–250. [[CrossRef](#)]
10. Hayes, R.; Warr, G.G.; Atkin, R. Structure and nanostructure in ionic liquids. *Chem. Rev.* **2015**, *115*, 6357–6426. [[CrossRef](#)]
11. Wang, S.; Wang, X. Imidazolium ionic liquids, imidazolyliene heterocyclic carbenes, and zeolitic imidazolate frameworks for CO₂ capture and photochemical reduction. *Angew. Chem. Int. Ed.* **2016**, *55*, 2308–2320. [[CrossRef](#)] [[PubMed](#)]
12. Egorova, K.S.; Gordeev, E.G.; Ananikov, V.P. Biological activity of ionic liquids and their application in pharmaceuticals and medicine. *Chem. Rev.* **2017**, *117*, 7132–7189. [[CrossRef](#)] [[PubMed](#)]
13. Dai, C.; Zhang, J.; Huang, C.; Lei, Z. Ionic liquids in selective oxidation: Catalysts and solvents. *Chem. Rev.* **2017**, *117*, 6929–6983. [[CrossRef](#)]
14. Basile, A.; Hilder, M.; Makhlooghiazad, F.; Pozo-Gonzalo, C.; MacFarlane, D.R.; Howlett, P.C.; Forsyth, M. Ionic liquids and organic ionic plastic crystals: Advanced electrolytes for safer high performance sodium energy storage technologies. *Adv. Energy Mater.* **2018**, *8*, 1703491. [[CrossRef](#)]
15. Gomes, J.M.; Silva, S.S.; Reis, R.L. Biocompatible ionic liquids: Fundamental behaviours and applications. *Chem. Soc. Rev.* **2019**, *48*, 4317–4335. [[CrossRef](#)] [[PubMed](#)]
16. Yoshida, Y.; Saito, G. Design of functional ionic liquids using magneto- and luminescent-active anions. *Phys. Chem. Chem. Phys.* **2010**, *12*, 1675–1684. [[CrossRef](#)] [[PubMed](#)]
17. Santos, E.; Albo, J.; Irabien, A. Magnetic ionic liquids: Synthesis, properties and applications. *RSC Adv.* **2014**, *4*, 40008–40018. [[CrossRef](#)]
18. Estager, J.; Holbrey, J.D.; Swadzba-Kwasny, M. Halometallate ionic liquids—revisited. *Chem. Soc. Rev.* **2014**, *43*, 847–886. [[CrossRef](#)]

19. Clark, K.D.; Nacham, O.; Purslow, J.A.; Pierson, S.A.; Anderson, J.L. Magnetic ionic liquids in analytical chemistry: A review. *Anal. Chim. Acta* **2016**, *934*, 9–21. [\[CrossRef\]](#)
20. Joseph, A.; Zyla, G.; Thomas, V.I.; Nair, P.R.; Padmanabhan, A.S.; Mathew, S. Paramagnetic ionic liquids for advanced applications: A review. *J. Mol. Liq.* **2016**, *218*, 319–331. [\[CrossRef\]](#)
21. Guerrero-Sanchez, C.; Lara-Ceniceros, T.; Jimenez-Regalado, E.; Raša, M.; Schubert, U.S. Magnetorheological fluids based on ionic liquids. *Adv. Mater.* **2007**, *19*, 1740–1747. [\[CrossRef\]](#)
22. Dodbiba, G.; Park, H.S.; Okaya, K.; Fujita, T. Investigating magnetorheological properties of a mixture of two types of carbonyl iron powders suspended in an ionic liquid. *J. Magn. Magn. Mater.* **2008**, *320*, 1322–1327. [\[CrossRef\]](#)
23. De Vicente, J.; Klingenberg, D.J.; Hidalgo-Alvarez, R. Magnetorheological fluids: A review. *Soft Matter* **2011**, *7*, 3701–3710. [\[CrossRef\]](#)
24. Kozlova, S.A.; Verevkin, S.P.; Heintz, A.; Peppel, T.; Köckerling, M. Paramagnetic ionic liquid 1-Butyl-3-methylimidazolium tetrabromidocobaltate(II): Activity coefficients at infinite dilution of organic solutes and crystal structure. *J. Chem. Eng. Data* **2009**, *54*, 1524–1528. [\[CrossRef\]](#)
25. Peppel, T.; Köckerling, M.; Geppert-Rybczyńska, M.; Ralys, R.V.; Lehmann, J.K.; Verevkin, S.P.; Heintz, A. Low-viscosity paramagnetic ionic liquids with doubly charged $[\text{Co}(\text{NCS})_4]^{2-}$ ions. *Angew. Chem. Int. Ed.* **2010**, *49*, 7116–7119. [\[CrossRef\]](#)
26. Geppert-Rybczyńska, M.; Lehmann, J.K.; Peppel, T.; Köckerling, M.; Heintz, A. Studies of physicochemical and thermodynamic properties of the paramagnetic 1-Alkyl-3-methylimidazolium ionic liquids $(\text{EMIm})_2[\text{Co}(\text{NCS})_4]$ and $(\text{BMIm})_2[\text{Co}(\text{NCS})_4]$. *J. Chem. Eng. Data* **2010**, *55*, 5534–5538. [\[CrossRef\]](#)
27. Peppel, T.; Köckerling, M. Salts with the 1,3-Dibutyl-2,4,5-trimethyl-imidazolium cation: $(\text{DBTMIm})\text{X}$ ($\text{X} = \text{Br}, \text{PF}_6$) and $(\text{DBTMIm})_2[\text{MBr}_4]$ ($\text{M} = \text{Co}, \text{Ni}$). *Z. Anorg. Allg. Chem.* **2010**, *636*, 2439–2446. [\[CrossRef\]](#)
28. Peppel, T.; Köckerling, M. Investigations on a series of ionic liquids containing the $[\text{Co}^{\text{II}}\text{Br}_3\text{quin}]^-$ anion (quin = quinoline). *Cryst. Growth Des.* **2011**, *11*, 5461–5468. [\[CrossRef\]](#)
29. Peppel, T.; Schmidt, C.; Köckerling, M. Synthesis, properties, and structures of salts with the reineckate anion, $[\text{Cr}^{\text{III}}(\text{NCS})_4(\text{NH}_3)_2]^-$, and large organic cations. *Z. Anorg. Allg. Chem.* **2011**, *637*, 1314–1321. [\[CrossRef\]](#)
30. Peppel, T.; Thiele, P.; Köckerling, M. Low-melting salts with the $[\text{Cr}^{\text{III}}(\text{NCS})_4(1,10\text{-Phenanthroline})]^-$ complex anion: Syntheses, properties, and structures. *Russ. J. Coord. Chem.* **2012**, *38*, 207–218. [\[CrossRef\]](#)
31. Peppel, T.; Hinz, A.; Köckerling, M. Salts with the $[\text{NiBr}_3(\text{L})]^-$ complex anion ($\text{L} = 1\text{-methylimidazole}, 1\text{-methylbenzimidazole}, \text{quinoline}, \text{and triphenylphosphane}$) and low melting points: A comparative study. *Polyhedron* **2013**, *52*, 482–490. [\[CrossRef\]](#)
32. Peppel, T.; Thiele, P.; Tang, M.-B.; Zhao, J.-T.; Köckerling, M. Low-melting imidazolium-based salts with the paramagnetic Reineckate-analogue anion $[\text{Cr}(\text{NCS})_4(\text{bipy})]^-$ (bipy = 2,2'-Bipyridine): Syntheses, properties, and structures. *Inorg. Chem.* **2015**, *54*, 982–988. [\[CrossRef\]](#) [\[PubMed\]](#)
33. Hensel-Bielowka, S.; Wojnarowska, Z.; Dzida, M.; Zorębski, E.; Zorębski, M.; Geppert-Rybczyńska, M.; Peppel, T.; Grzybowska, K.; Wang, Y.; Sokolov, A.P.; et al. Heterogeneous nature of relaxation dynamics of room-temperature ionic liquids $(\text{EMIm})_2[\text{Co}(\text{NCS})_4]$ and $(\text{BMIm})_2[\text{Co}(\text{NCS})_4]$. *J. Phys. Chem. C* **2015**, *119*, 20363–20368. [\[CrossRef\]](#)
34. Peppel, T.; Hinz, A.; Thiele, P.; Geppert-Rybczyńska, M.; Lehmann, J.K.; Köckerling, M. Synthesis, properties, and structures of low-melting tetrakisocyanatocobaltate(II)-based ionic liquids. *Eur. J. Inorg. Chem.* **2017**, 885–893. [\[CrossRef\]](#)
35. Pincussohn, L. Über die metallverbindungen des pyridins und die elektrolyse des pyridins. *Z. Anorg. Allg. Chem.* **1897**, *14*, 379–403. [\[CrossRef\]](#)
36. Reitzenstein, F. Ammoniak-pyridinsalze und hydrate bivalenter metalle. *Z. Anorg. Allg. Chem.* **1898**, *18*, 253–304. [\[CrossRef\]](#)
37. Taylor, F.S. The manganohalides of pyridine and quinoline. *J. Chem. Soc.* **1934**, 699–701. [\[CrossRef\]](#)
38. Jørgensen, C.K. Comparative ligand field studies. III. The decrease of the integral F^k for manganese(II) complexes as evidence for partly covalent bonding. *Acta Chem. Scand.* **1957**, *11*, 53–72. [\[CrossRef\]](#)
39. Gill, N.S.; Nyholm, R.S.; Pauling, P. Stereochemistry of complex halides of the transition metals. *Nature* **1958**, *182*, 168–170. [\[CrossRef\]](#)
40. Buffagni, S.; Dunn, T.M. Spectra of tetrahedral inorganic complexes. *Nature* **1960**, *188*, 937–938. [\[CrossRef\]](#)
41. Cotton, F.A.; Goodgame, D.M.L.; Goodgame, M. Absorption spectra and electronic structures of some tetrahedral manganese(II) complexes. *J. Am. Chem. Soc.* **1962**, *84*, 167–172. [\[CrossRef\]](#)

42. Forster, D.; Goodgame, D.M.L. Preparation, electronic spectra, and magnetic properties of some transition-metal Isocyanato-complexes. *J. Chem. Soc.* **1964**, 2790–2798. [[CrossRef](#)]
43. Cotton, F.A.; Daniels, L.M.; Huang, P. Correlation of structure and triboluminescence for tetrahedral manganese(II) compounds. *Inorg. Chem.* **2001**, *40*, 3576–3578. [[CrossRef](#)] [[PubMed](#)]
44. Pitula, S.; Mudring, A.-V. Synthesis, structure, and physico-optical properties of manganate(II)-based ionic liquids. *Chem. Eur. J.* **2010**, *16*, 3355–3365. [[CrossRef](#)] [[PubMed](#)]
45. Zhang, H.; Chen, P.; Fang, L. Hexaimidazolium tetrachloromanganate(II) hexachloromanganate(II). *Acta Cryst.* **2006**, *E62*, m658–m660. [[CrossRef](#)]
46. Chang, J.-C.; Ho, W.-Y.; Sun, I.-W.; Chou, Y.-K.; Hsieh, H.-H.; Wu, T.-Y. Synthesis and properties of new tetrachlorocobaltate(II) and tetrachloromanganate(II) anion salts with dicationic counterions. *Polyhedron* **2011**, *30*, 497–507. [[CrossRef](#)]
47. Zhong, C.; Sasaki, T.; Jimbo-Kobayashi, A.; Fujiwara, E.; Kobayashi, A.; Tada, M.; Iwasawa, Y. Syntheses, structures, and properties of a series of metal ion-containing dialkylimidazolium ionic Liquids. *Bull. Chem. Soc. Jpn.* **2007**, *80*, 2365–2374. [[CrossRef](#)]
48. Zehbe, K.; Kolloosche, M.; Lardong, S.; Kelling, A.; Schilde, U.; Taubert, A. Ionogels based on poly(methyl methacrylate) and metal-containing ionic liquids: Correlation between structure and mechanical and electrical properties. *Int. J. Mol. Sci.* **2016**, *17*, 391. [[CrossRef](#)]
49. Del Sesto, R.E.; McCleskey, T.M.; Burrell, A.K.; Baker, G.A.; Thompson, J.D.; Scott, B.L.; Wilkes, J.S.; Williams, P. Structure and magnetic behavior of transition metal based ionic liquids. *Chem. Commun.* **2008**, 447–449. [[CrossRef](#)]
50. Lokanath, N.K.; Sridhar, M.A.; Shashidhara Prasad, J. Crystal structure of metoclopramide manganese isothiocyanate complex. *Z. Krist. New. Cryst. Struct.* **1997**, *212*, 19–20.
51. Chen, H.-J.; Zhang, L.-Z.; Cai, Z.-G.; Yang, G.; Chen, X.-M. Organic–inorganic hybrid materials assembled through weak intermolecular interactions. Synthesis, structures and non-linear optical properties of $[4,4'\text{-bipyH}_2][\text{M}(\text{NCS})_4]$ ($\text{M} = \text{Mn}^{2+}$, Co^{2+} or Zn^{2+} ; 4,4'-bipy = 4,4'-bipyridine). *J. Chem. Soc. Dalton Trans.* **2000**, 2463–2466. [[CrossRef](#)]
52. Kushch, N.D.; Bardin, A.A.; Buravov, L.I.; Glushakova, N.M.; Shilov, G.V.; Dmitriev, A.I.; Morgunov, R.B.; Kulikov, A.V. Synthesis particularities, structure and properties of the radical cation salts $\omega\text{-(BEDT-TTF)}_5\text{M}(\text{NCS})_6\cdot\text{C}_2\text{H}_5\text{OH}$, $\text{M} = \text{Mn}$, Ni . *Synth. Met.* **2014**, *195*, 75–82. [[CrossRef](#)]
53. Neumann, T.; Jess, I.; Nather, C. Crystal structures of bis-[4-(di-methyl-amino)-pyridinium] tetra-kis-(thio-cyanato- κN)manganate(II) and tris-[4-(di-methyl-amino)-pyridinium] penta-kis(thio-cyanato- κN)manganate(II). *Acta Cryst.* **2017**, *E73*, 1786–1789.
54. Thuyweang, N.; Koh, L.L.; Hor, T.S.A.; Leelasubcharoen, S. Synthesis, characterization, and catalytic activity of heterometallic ion-pair Ni/Mn and Ni/Zn complexes. *J. Coord. Chem.* **2014**, *67*, 1219–1235. [[CrossRef](#)]
55. Fulmer, G.R.; Miller, A.J.M.; Sherden, N.H.; Gottlieb, H.E.; Nudelman, A.; Stoltz, B.M.; Bercaw, J.E.; Goldberg, K.I. NMR chemical shifts of trace impurities: Common laboratory solvents, organics, and gases in deuterated solvents relevant to the organometallic chemist. *Organometallics* **2010**, *29*, 2176–2179. [[CrossRef](#)]
56. Bruker AXS Inc. *Apex-2*, v. 1.6–8, Saint, v. 6.25a, SADABS—Software for the CCD Detector System; Bruker-Nonius Inc.: Madison, WI, USA, 2003.
57. Sheldrick, G. A short history of SHELX. *Acta Crystallogr. Sect. A* **2008**, *64*, 112–122. [[CrossRef](#)]
58. Evans, D.F. The determination of the paramagnetic susceptibility of substances in solution by nuclear magnetic resonance. *J. Chem. Soc.* **1959**, 2003–2005. [[CrossRef](#)]
59. Sur, S.K. Measurement of magnetic susceptibility and magnetic moment of paramagnetic molecules in solution by high-field fourier transform NMR spectroscopy. *J. Magn. Reson.* **1989**, *82*, 169–173. [[CrossRef](#)]
60. Pacault, A.; Hoarau, J.; Marchand, A. New views of diamagnetism. *Adv. Chem. Phys.* **1960**, *3*, 171–238.
61. Langevin, P. Magnétisme et théorie des électrons. *Ann. Chim. Phys.* **1905**, *8*, 70–127.
62. Wandschneider, A.; Lehmann, J.K.; Heintz, A. Surface tension and density of pure ionic liquids and some binary mixtures with 1-propanol and 1-butanol. *J. Chem. Eng. Data* **2008**, *53*, 596–599. [[CrossRef](#)]
63. Huddleston, J.G.; Visser, A.E.; Reichert, W.M.; Willauer, H.D.; Broker, G.A.; Rogers, R.D. Characterization and comparison of hydrophilic and hydrophobic room temperature ionic liquids incorporating the imidazolium cation. *Green Chem.* **2001**, *3*, 156–164. [[CrossRef](#)]
64. Padilla-Martinez, I.I.; Ariza-Castolo, A.; Contreras, R. NMR study of isolobal N-CH_3^+ , N-BH_3 and N-BF_3 imidazole derivatives. *Magn. Reson. Chem.* **1993**, *31*, 189–193. [[CrossRef](#)]

65. Forster, D.; Goodgame, D.M.L. Electronic spectra and magnetic properties of some isothiocyanate complexes of manganese and iron. *J. Chem. Soc.* **1965**, 268–274. [[CrossRef](#)]
66. Nishida, T.; Tashiro, Y.; Yamamoto, M. Physical and electrochemical properties of 1-alkyl-3-methylimidazolium tetrafluoroborate for electrolyte. *J. Fluor. Chem.* **2003**, *120*, 135–141. [[CrossRef](#)]
67. Namboodiri, V.V.; Varma, R.S. Solvent-free sonochemical preparation of ionic liquids. *Org. Lett.* **2002**, *4*, 3161–3163. [[CrossRef](#)]
68. Earle, M.; Seddon, K.R. Light Emitting Complex Salts. Patent WO 2006/043110 A1, 27 April 2006.
69. Sabatini, A.; Bertini, I. Infrared spectra between 100 and 2500 cm^{-1} of some complex metal cyanates, thiocyanates, and selenocyanates. *Inorg. Chem.* **1965**, *4*, 959–961. [[CrossRef](#)]
70. Kauzmann, W. The nature of the glassy state and the behavior of liquids at low temperatures. *Chem. Rev.* **1948**, *43*, 219–256. [[CrossRef](#)]
71. Lee, W.A.; Knight, G.J. Ratio of the glass transition temperature to the melting point in polymers. *Br. Polym. J.* **1970**, *2*, 73–80. [[CrossRef](#)]
72. Widegren, J.A.; Laesecke, A.; Magee, J.W. The effect of dissolved water on the viscosities of hydrophobic room-temperature ionic liquids. *Chem. Commun.* **2005**, 1610–1612. [[CrossRef](#)]
73. Jacquemin, J.; Husson, P.; Padua, A.A.H.; Majer, V. Density and viscosity of several pure and water-saturated ionic liquids. *Green Chem.* **2006**, *8*, 172–180. [[CrossRef](#)]
74. Tariq, M.; Freire, M.G.; Saramago, B.; Coutinho, J.A.P.; Canongia Lopes, J.N.; Rebelo, L.P.N. Surface tension of ionic liquids and ionic liquid solutions. *Chem. Soc. Rev.* **2012**, *41*, 829–868. [[CrossRef](#)]
75. Dzida, M.; Zorębski, E.; Zorębski, M.; Żarska, M.; Geppert-Rybczyńska, M.; Chorażewski, M.; Jacquemin, J.; Cibulka, I. Speed of sound und ultrasound absorption in ionic liquids. *Chem. Rev.* **2017**, *117*, 3883–3929. [[CrossRef](#)] [[PubMed](#)]
76. Feder-Kubis, J.; Musiał, M.; Dizda, M.; Geppert-Rybczyńska, M. The new evolution of protic ionic liquids: Antielectrostatic activity correlated with their surface properties. *J. Ind. Eng. Chem.* **2016**, *41*, 40–49. [[CrossRef](#)]
77. Yaghini, N.; Nordstierna, L.; Martinelli, A. Effect of water on the transport properties of protic and aprotic imidazolium ionic liquids—An analysis of self-diffusivity, conductivity, and proton exchange mechanism. *Phys. Chem. Chem. Phys.* **2014**, *16*, 9266–9275. [[CrossRef](#)] [[PubMed](#)]
78. Vogel, H. Das temperaturabhängigkeitsgesetz der viskosität von flüssigkeiten. *Phys. Z.* **1921**, *22*, 645–646.
79. Fulcher, G.S. Analysis of recent measurements of the viscosity of glasses. *J. Am. Ceram. Soc.* **1925**, *8*, 339–355. [[CrossRef](#)]
80. Tammann, G.; Hesse, W. Die abhängigkeit der viscosität von der temperatur bei unterkühlten flüssigkeiten. *Z. Anorg. Allg. Chem.* **1926**, *156*, 245–257. [[CrossRef](#)]



© 2019 by the authors. Licensee MDPI, Basel, Switzerland. This article is an open access article distributed under the terms and conditions of the Creative Commons Attribution (CC BY) license (<http://creativecommons.org/licenses/by/4.0/>).